

EFFECT OF DOPING WITH COPPER (II) AND NICKEL (II) OXIDES ON MORPHOLOGICAL PROPERTIES OF SILICA/TITANIA NANOCOMPOSITES

M.A. Nazarkovsky ^{1*}, E.V. Goncharuk ¹, E.M. Pakhlov ¹, E. Skwarek ²,
J. Skubiszewska-Zięba ², R. Leboda ², W. Janusz ², V.M. Gun'ko ¹

¹ *Chuiko Institute of Surface Chemistry of National Academy of Sciences of Ukraine
17 General Naumov Str., Kyiv, 03164, Ukraine*

² *Maria Curie-Skłodowska University, Faculty of Chemistry
3 Maria Curie-Skłodowska pl., Lublin, 20031, Poland*

Morphological characteristics of CuO- and NiO-doped silica/titania nanocomposites are analyzed using atomic force microscopy and low-temperature nitrogen adsorption. The different types of pores (nano-, meso- and macropores) in the powder composites are modeled as voids between spherical nanoparticles packed in random aggregates. It is shown that specific surface area, total pore volume, average pore radius, incremental pore size distribution and changes in relationships between these characteristics of the composites reveal a non-linear behavior depended on the presence of the dopants. The textural and atomic force microscopy investigations suggest that processes of aggregation differ from each other depending on the type of doping oxide. Fractal dimension, estimated according to Frenkel-Halsey-Hill equation using the adsorption branch, has values about 2.50–2.60 and indicates the aggregate formation.

INTRODUCTION

Varying the content and types of dopants in composite nanomaterials based on different matrices (silica or titania) affects changes in their morphology and allows one to produce new redox or acid/base catalysts and photocatalysts with required properties for specific applications [1–10]. The textural characteristics of composites depend on properties of both dopant (acidity, bandgap value) and matrix (textural and electronic characteristics). For instance, specific surface area, S_{BET} , and total pore volume, V_p , distinctly depend on the type of dopant, including NiO and CuO, into the silica matrix [8]. The incremental pore size distribution (IPSD) profiles differ for pure nanosilicas and nanocomposites containing Al_2O_3 that can be caused by changes in interactions between primary particles due to presence of alumina and silica on the composite surface [9]. Hence, the character of the primary nanoparticles packing changes too. TiO_2 -containing silicas demonstrated diminution of the S_{BET} value with increasing concentration of titania.

This paper focuses on titania-silica composites doped with nickel(II) or copper(II)

oxides. The aim was to investigate the morphological properties of synthesized mixed oxides dependent of deposited dopant type and content. Low-temperature N_2 adsorption-desorption has been used for this purpose and all calculated parameters (S_{BET} , V_p , R_p , IPSD_V , contributions of different pores types) and relationships between them are analyzed, as well as atomic force microscopy (AFM) images.

The topography and roughness of a surface of many solid systems can be characterized by the surface fractal dimension D_s [11, 12] which is a kind of roughness parameters. The D_s value for the ideal flat surface is equal to 2 but for a real irregular surface D_s can vary between 2 and 3 and expresses so the degree of roughness of the surface and porous structures like oxide nanocomposites. Additionally, fractal dimension of fumed oxides reflects both mass fractal dimension and textural pore fractal dimension. Thus, the D_s values analyzed here can be considered as an integral measure of nanooxide fractality.

AFM images are helpful to identify certain characteristics of aggregates of nanoparticles and agglomerates of aggregates because the structural hierarchy of nanocomposites depends on both their composition and synthesis method.

* corresponding author nazarkovsky.michael@gmail.com

MATERIAL AND METHODS

The nanocomposites were obtained using low-temperature hydrolysis of precursors for sequentially depositing of CuO and NiO as dopants and TiO₂ as a functional phase onto the nanosilica surface. The synthesis was carried out in a glass reactor equipped by a mechanical Teflon stirrer, an air blow-through emitter device and a heating system. Nanosilica A-300 (50 g, $S_{\text{BET}} = 294 \text{ m}^2/\text{g}$ produced at pilot plant at Chuiko Institute of Surface Chemistry, Kalush, Ukraine) was added into the reactor after heating (6 h at 450 °C), whereat enough for hydrolysis portion of water was added within stirring at room temperature. In 1 h saturated solution of Cu(CH₃CO₂)₂, H₂O (Merck KGaA, Germany) was added to form CuO from 0.14 up to 30 wt. % against TiO₂. Then in 0.5 h TiCl₄ (Merck KGaA, Germany) was injected into the mixture to generate TiO₂-phase in 15 wt. % against nanosilica matrix. After all the reagents had been added, the system was heated up to 100 °C and thermally treated during 1.5 h stirred. To remove HCl the reactor has been blown through by the air stream for 1 h. Finally the mixture was cooled off to the room temperature.

NiO-doped composites (0.14–30.0 wt. % against TiO₂) were obtained by treatment of saturated Ni(NO₃)₂ solution at 20 °C on the A-300 surface. As in the previous case the amount of water contained in the crystalline hydrate Ni(NO₃)₂·6H₂O was taken into account by solution preparing. As in the case with SiO₂/TiO₂/CuO composite synthesis described above TiCl₄ was added in a half hour's lapse to make TiO₂ (15 wt. % against nanosilica matrix). The mixture in the reactor was heated up to 100 °C and kept during 1.5 h stirred before blowing-through by the air stream for 1 h and cooling off to the room temperature.

All obtained composites were heated at 100 °C during 3 h to remove residual water and HCl and then ones were being calcined at 600 °C for 6 h until anatase as a crystalline phase of TiO₂ was formed.

The composition and morphological characteristics of the nanocomposites are presented in Table 1. To determine and analyze the morphological properties of synthesized nanocomposites, low-temperature nitrogen adsorption-desorption isotherms were recorded

using a Micromeritics ASAP 2405N adsorption analyzer. The specific surface area was calculated according to the standard BET method [13, 14]. The total pore volume was estimated from the nitrogen adsorption data at the relative pressure $p/p_0 \approx 0.98\text{--}0.99$. To compute the pore size distributions, the desorption data were used. The proposed computation is based on use of regularization procedure under non-negativity condition for the pore size distribution function ($f(R_p) > 0$ at any pore radius R_p) at fixed regularization parameter $\alpha = 0.01$. The pores as the voids between spherical nanoparticles packed in random aggregates ($d < 1 \mu\text{m}$, [14]) are considered. This approach based on Nguen-Do method developed for porous carbons [15, 16] was modified to be used for a variety of nanomaterials [8, 17–19]. The functions $f_v(R_p)$ and $f_s(R_p)$ were used to get contributions of different types of pores: nanopores (V_{nano} , S_{nano} at $R_p < 1 \text{ nm}$), mesopores (V_{meso} , S_{meso} at $1 \text{ nm} \leq R_p \leq 25 \text{ nm}$) and macropores (V_{macro} , S_{macro} , $R_p > 25 \text{ nm}$) [20]. To verify the chosen pore model criterion Δw is used [21]

$$\Delta w = \frac{S_{\text{BET}}}{R_{\text{max}} \int_{R_{\text{min}}} f_s(R_p) dR_p} - 1. \quad (1)$$

The Eq.(1) represents condition of right use of the mentioned above model.

The estimation of nanooxide fractality was performed on the basis the Frenkel-Halsey-Hill (FHH) method described in detail by Avnir and Jaroniec [22] which can be applied in the range of multilayer adsorption. For this purpose the adsorption branch within $p/p_0 = 0.01\text{--}0.8$ values has been used where attraction between adsorbent and adsorbate is caused chiefly by van der Waals forces [22–24]. D_s can be calculated from the plot corresponding to the Eq. (2):

$$\ln(V/V_0) = (D_s - 3) \cdot \ln[\ln(p_0/p)] + \text{const}, \quad (2)$$

where V , V_0 are the adsorbed volume of N₂, the saturation volume of adsorbed N₂, respectively, p and p_0 are the equilibrium and saturation pressure of nitrogen adsorbed, respectively.

The particle morphology has been studied using AFM (NanoScope V, Veeco, USA) with 5120×5120 pixel density and separative power of 0.1 nm.

RESULTS AND DISCUSSION

The nitrogen adsorption-desorption isotherms obtained for both types of composites with $\text{SiO}_2/\text{TiO}_2/\text{CuO}$ and $\text{SiO}_2/\text{TiO}_2/\text{NiO}$ demonstrate the hysteresis loops of H3 type (Fig. 1) [13]. That indicates the formation of aggregates with nonporous nanoparticles that are characterized by the textural porosity (the loops are narrow and their onset is at $p/p_0 = 0.8-0.9$). This also causes the isotherm shapes corresponding to type II of the IUPAC classification of pores. Fig. 1 shows different character of adsorption ability of composites since the highest values are reached within 0.14–5 wt. % of CuO and there is a high ability of the $\text{SiO}_2/\text{TiO}_2/\text{NiO}$ system with except at $C_{\text{NiO}} = 5$ wt. %. This is due two opposite effects such as the formation of smaller nanoparticles than the matrix ones (increasing textural parameters) but of larger specific density than that of silica (decreasing textural parameters).

It is shown that the Δw values (Table 1) reveal an agreement between the proposed model

of pores and their real structure since the errors are smaller than 20 %. Notice that the highest Δw values are observed at the maximal dopants concentrations in the both systems. This fact supports the supposition that very high concentrated dopants bring more significant changes in the shape of nanoparticles and their aggregates, e.g. the nanoparticles become less spherical and aggregates are more strongly compacted.

According to Table 1, the S_{BET} value as function of dopant concentration has different profiles dependent on the type of doping metal oxide (Fig. 2). The loss of S_{BET} is a result of complex processes occurred on the nanosilica surface by consecutive introduction of CuO or NiO and TiO_2 . Therefore, there is the non-linear dependence on CuO or NiO concentration. At minimal concentrations, the loss of S_{BET} in both systems is hardly observed since in the case of NiO-containing one there is almost no change in the S_{BET} value compared to the initial nanosilica ($S_{\text{BET}} = 294 \text{ m}^2/\text{g}$).

Table 1. Morphological characteristics of synthesized CuO- and NiO-doped silica-titania composites

Sample	$S_{\text{BET}}, \text{m}^2/\text{g}$	$S_{\text{nano}}, \text{m}^2/\text{g}$	$S_{\text{meso}}, \text{m}^2/\text{g}$	$S_{\text{macro}}, \text{m}^2/\text{g}$	$V_p, \text{cm}^3/\text{g}$	$V_{\text{nano}}, \text{cm}^3/\text{g}$	$V_{\text{meso}}, \text{cm}^3/\text{g}$	$V_{\text{macro}}, \text{cm}^3/\text{g}$	R_p, nm	Δw
$\text{SiO}_2/\text{TiO}_2/\text{CuO}$ $\omega(\text{CuO}) = 0.14$ wt. %	289.2	23.9	258.3	7.0	0.714	0.009	0.615	0.090	12.8	-0.044
$\text{SiO}_2/\text{TiO}_2/\text{CuO}$ $\omega(\text{CuO}) = 1$ wt. %	244.5	5.1	200.5	38.9	1.100	0.002	0.504	0.593	24.4	0.059
$\text{SiO}_2/\text{TiO}_2/\text{CuO}$ $\omega(\text{CuO}) = 5$ wt. %	278.4	15.8	238.7	24.0	0.980	0.006	0.643	0.331	18.7	-0.010
$\text{SiO}_2/\text{TiO}_2/\text{CuO}$ $\omega(\text{CuO}) = 10$ wt. %	256.3	10.0	216.9	29.4	0.965	0.004	0.533	0.428	21.5	0.032
$\text{SiO}_2/\text{TiO}_2/\text{CuO}$ $\omega(\text{CuO}) = 30$ wt. %	250.6	17.3	220.5	12.8	0.581	0.007	0.380	0.193	15.6	-0.249
$\text{SiO}_2/\text{TiO}_2/\text{NiO}$ $\omega(\text{NiO}) = 0.14$ wt. %	293.8	10.2	269.5	14.1	0.904	0.004	0.710	0.190	16.2	-0.036
$\text{SiO}_2/\text{TiO}_2/\text{NiO}$ $\omega(\text{NiO}) = 1$ wt. %	296.8	8.4	276.1	12.3	0.877	0.004	0.715	0.158	15.8	-0.039
$\text{SiO}_2/\text{TiO}_2/\text{NiO}$ $\omega(\text{NiO}) = 5$ wt. %	290.7	25.7	262.0	3.0	0.559	0.010	0.510	0.039	9.69	-0.029
$\text{SiO}_2/\text{TiO}_2/\text{NiO}$ $\omega(\text{NiO}) = 10$ wt. %	265.6	11.9	233.1	20.7	0.878	0.005	0.687	0.308	17.8	-0.027
$\text{SiO}_2/\text{TiO}_2/\text{NiO}$ $\omega(\text{NiO}) = 30$ wt. %	258.6	1.6	251.8	5.2	0.813	0.001	0.752	0.061	13.8	0.191

At $C_{\text{CuO}} = 5$ wt. %, a maximum corresponds to the loss of 7 % S_{BET} only. But at $C_{\text{dop}} = 1$ % there is a dramatic difference in S_{BET} changes since NiO provokes an increase but CuO gives 18.5 % loss greater than that at its maximal

concentration (16.5 %). At $C_{\text{NiO}} = 30$ wt. % the specific surface area loses 14.5 %.

The analyzed dependence allows us to assume that the nanoparticles of NiO-doped system are smaller than those of $\text{SiO}_2/\text{TiO}_2/\text{CuO}$ at the same concentrations. The biggest

contribution to S_{BET} is made by mesopores in both cases but their part in $SiO_2/TiO_2/NiO$ is higher than in $SiO_2/TiO_2/CuO$ though a comparable character of profile change (Fig. 3), at $C_{dop} = 0.14$ and 30 wt. % there are most significant S_{meso} shares.

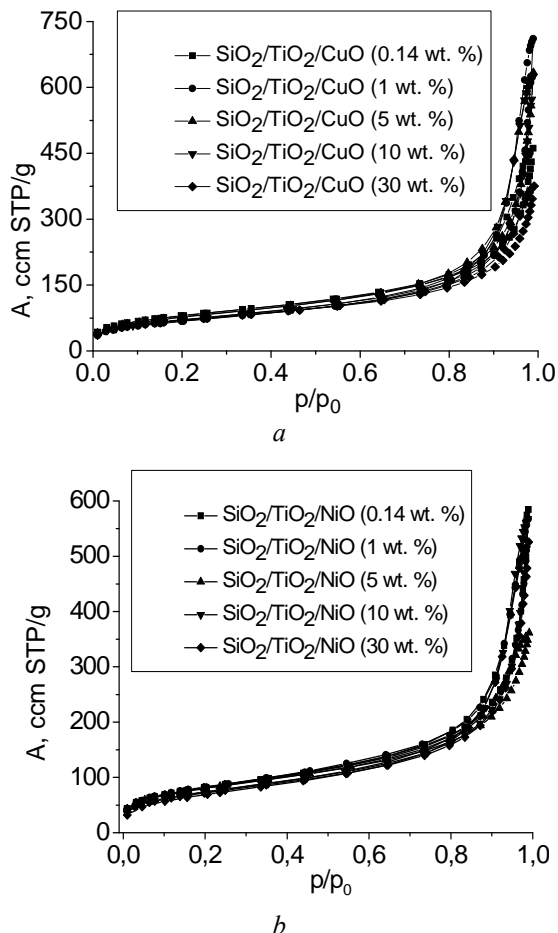


Fig. 1. Nitrogen adsorption-desorption isotherms for composites $SiO_2/TiO_2/CuO$ (a) and $SiO_2/TiO_2/NiO$ (b)

Given the fact that there is a sharp decrease in S_{BET} at $C_{CuO} = 1\%$ that can be explained by certain compaction of aggregates that causes an increase in contribution of macropores (voids between aggregates in agglomerates). At this concentration, a maximum of the function is observed (Fig. 4). Taking into account a similar behavior of the V_{macro} vs C_{dop} plot we have ground to assume that the aggregate/agglomerate systems possess the dopant-content dependent structure that can strongly affect the S_{BET} value (i.e. particle sizes and, therefore, their electronic structure and catalytic properties). The extremal character of the curves for $SiO_2/TiO_2/NiO$

(Figs. 4, a, b) is the key to explaining high values of S_{BET} kept at $C_{NiO} = 1-5$ wt. %.

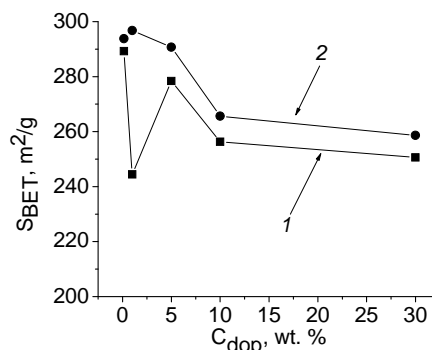


Fig. 2. Changes in the specific surface area of composites vs the dopant content (CuO-1, NiO-2)

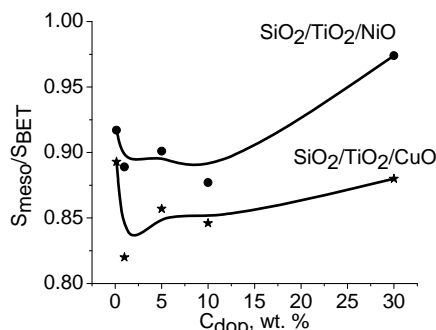


Fig. 3. Contribution of mesopores to total specific surface area vs. concentration of dopants

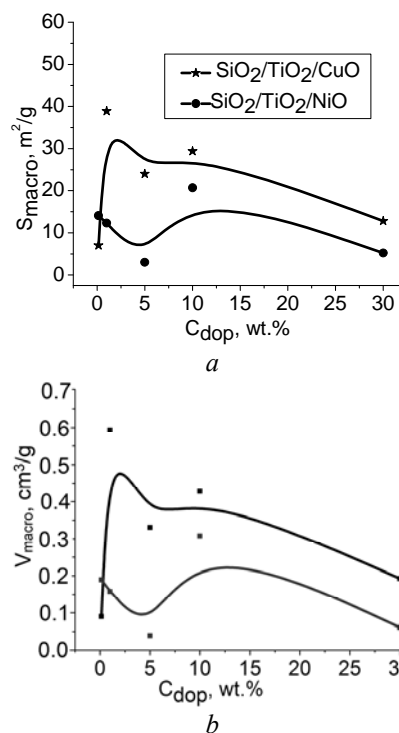


Fig. 4. Changes in S_{macro} (a) and V_{macro} (b) vs dopant concentration

It is obvious that total pore volume is due to contributions of mesopores and macropores since the V_{meso} and V_{macro} values much stronger contribute the V_p value than V_{nano} does but the absolute values differ from each other compared two nanooxide systems (Table 1, Fig. 5). Meanwhile V_p decreases with S_{BET} augmentation (Fig. 6, a) but $\text{SiO}_2/\text{TiO}_2/\text{CuO}$ samples demonstrate more intensive diminution and in our opinion that is provoked by stronger particle consolidation than in NiO-containing system.

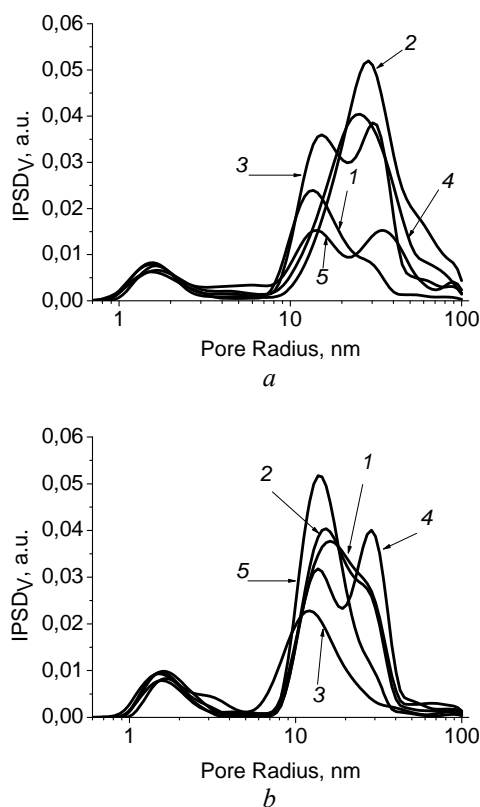


Fig. 5. IPSD_V of nanocomposites: $\text{SiO}_2/\text{TiO}_2/\text{CuO}$ (a) and $\text{SiO}_2/\text{TiO}_2/\text{NiO}$ (b): 0.14 wt. % (1), 1 wt. % (2), 5 wt. % (3), 10 wt. % (4), 30 wt. % (5)

We observe the same situation with R_p vs S_{BET} (Fig. 6, b). That fact is corroborated with results of AFM investigations since the images of $\text{SiO}_2/\text{TiO}_2/\text{CuO}$ (Fig. 7, d-f) indicate aggregates to be present having bigger sizes than in $\text{SiO}_2/\text{TiO}_2/\text{NiO}$ except sample at $C_{\text{NiO}} = 30$ wt. % where particles begin to build a compact structure (Fig. 7, c). As rule, hydrolytic stability of M-O-Si bonds (M-Cu, Ni) causes these sorts of structural effects [8].

This observation leads to conclusion that increase in concentration of both dopants results in

intensification of M-O-Si-bond stability and Cu-O-Si fragment is stronger than Ni-O-Si although both Ni and Cu belong to the “borderline acids” according to the HSAB concept [25], and their electronegativity values differ slightly: 1.9 and 1.91 acc. to Pauling [26], 1.85 and 1.88 acc. to Allen [27] for Cu and Ni, respectively.

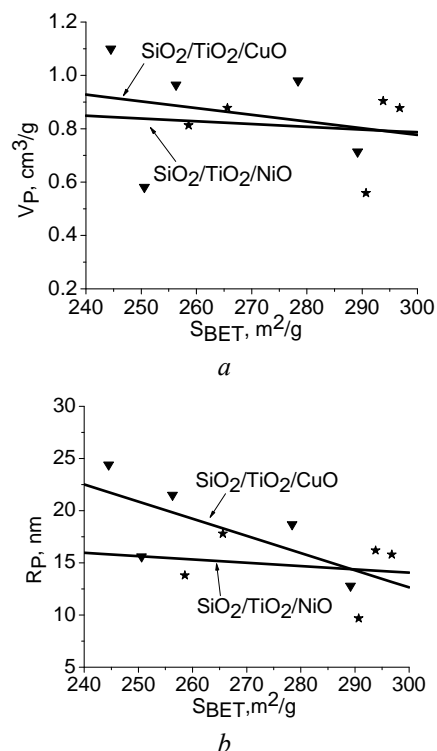


Fig. 6. Relationship between total pore volume V_p (a), average pore radius R_p (b) and specific surface area S_{BET}

Fractal dimension D_s calculated with the FHH method (Fig. 8, a, b) takes values from 2.56 to 2.59, i.e. these values are typical for nanooxides [22] and there is no essential changes in the surface roughness, aggregate/agglomerate organization and mass fractality of the composites with increasing CuO or NiO content. However, there are two contrary trends with different types of present dopants (Fig. 9). Weak positive tendency is stimulated by CuO opposite to the illustrated trend line of NiO-composite. These phenomena tend one to suggest that weak trends of the fractality with the whole range of explicit morphological transformations (IPSD_V , V_p and R_p) show that the shapes of voids stay immutable.

Thus, dopant's phase is deposited mostly in bulk instead of forming on the surface – otherwise fractalities of individual phases found on external layers could make changes in roughness in the larger scale.

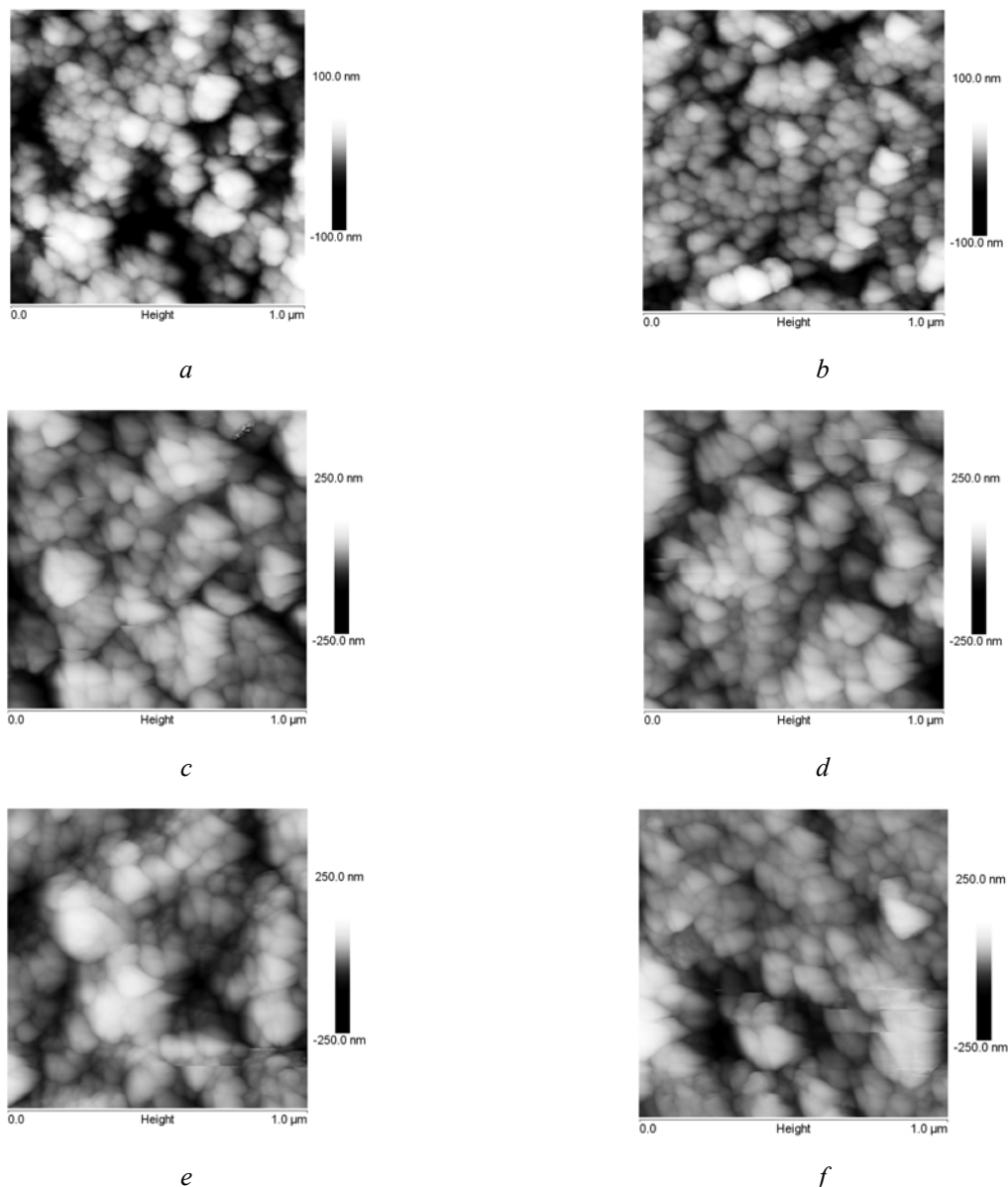


Fig. 7. AFM images of SiO₂/TiO₂/NiO (*a* – 0.14 wt. %, *b* – 10 wt. %, *c* – 30 wt. %) and SiO₂/TiO₂/CuO (*d* – 0.14 wt. %, *e* – 5 wt. %, *f* – 30 wt. %)

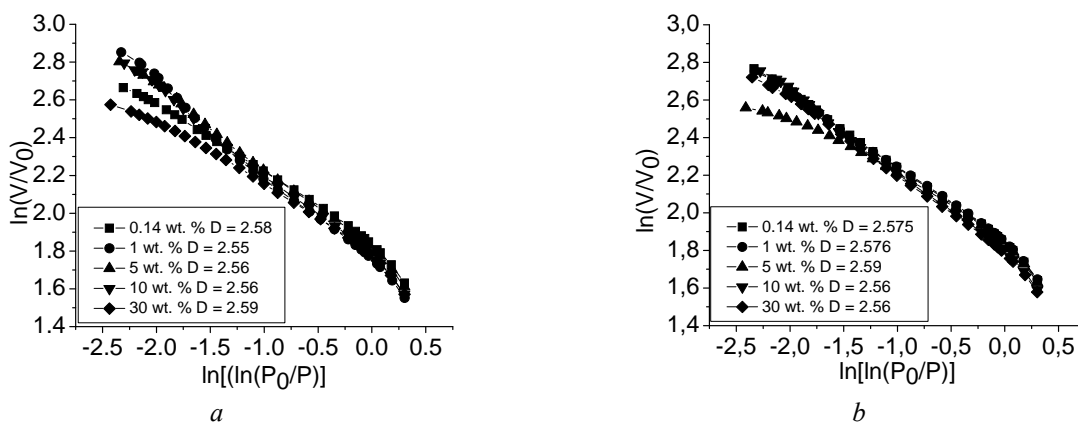


Fig. 8. Frenkel-Halsey-Hill plot for SiO₂/TiO₂/CuO (*a*) and SiO₂/TiO₂/NiO (*b*) composites

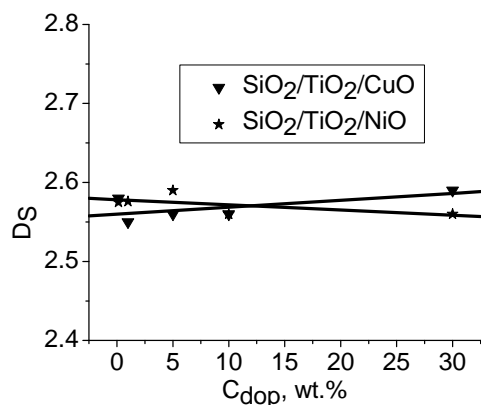


Fig. 9. Fractal dimension trends vs dopant concentrations in the composites

CONCLUSIONS

Low-temperature hydrolysis technique is used to produce CuO- and NiO-doped titania composites on the basis of nanosilica. Method of N₂ adsorption-desorption used to calculate the most important structural characteristics shows that features of S_{BET} changes have the extremal behavior within small amounts of introduced doping oxides, e.g. NiO promotes slight S_{BET} rise keeping its high value at 0.14–5 wt. % although such oxide systems are inclined to form strong aggregates and agglomerates very intensively. But augmentation of dopants' content stimulates S_{BET} fall.

Our results indicate that maximal contribution to S_{BET} and total pore volume V_p is made by meso- and macropores because nanoparticles are nonporous but voids between them correspond to meso- and macropores. Their shares are changed depending in the course of dopants concentration growing.

The main part of CuO and NiO is found in the bulk of obtained systems since the fractal dimension values are not subjected to significant change, i.e. surface roughness stays nearly constant.

The sizes of SiO₂/TiO₂/NiO particles are smaller than ones of SiO₂/TiO₂/CuO composites according to changes in the S_{BET} values and AFM images.

ACKNOWLEDGEMENTS

The authors are grateful to the European Community, Seventh Framework Programme (FP7/2007-2013), Marie Curie International Research Staff Exchange Scheme (grant N 230790) for financial support.

REFERENCES

1. Stark W.J., Strobel R., Günter D. et al. Titania-silica doped with transition metals via flame synthesis: structural properties and catalytic behavior in epoxidation // *J. Mat. Chem.* – 2002. – V. 12. – P. 3620–3625.
2. Othman S.H., Rashid S.A., Ghazi T.I.M., Abdullah N. Fe-doped TiO₂ nanoparticles produced via MOCVD: synthesis, characterization, and photocatalytic activity // *J. Nanomater.* – 2011. – V. 2011., ID 571601. – P. 1–8.
3. Zaleska A. Doped-TiO₂: A review // *Recent Patents on Engineering.* – 2008. – V. 2. – P. 157–164.
4. Tian B., Li Ch., Gu F. et al. Flame sprayed V-doped TiO₂ nanoparticles with enhanced photocatalytic activity under visible light irradiation // *Chem. Eng. J.* – 2009. – V. 151. – P. 220–227.
5. Gun'ko V.M., Blitz J.P., Zarko V.I. et al. Structural and adsorption characteristics and catalytic activity of titania and titania-containing nanomaterials // *J. Colloid Interface Sci.* – 2009. – V. 330. – P. 125–137.
6. Gun'ko V.M., Zarko V.I., Mironyuk I.F. et al. Surface electric and titration behavior of fumed oxides // *Colloids Surf. A.* – 2004. – V. 240. – P. 9–25.
7. Choi W., Termin A., Hoffmann M.R. The role of metal ion dopants in quantum-sized TiO₂: correlation between photoreactivity and charge carrier recombination dynamics // *J. Phys. Chem.* – 1994. – V. 98. – P. 13669–13679.
8. Gun'ko V.M., Bogatyrev V.M., Borysenko M.V. et al. Morphological, structural and adsorption features of oxide composites with silica and titania matrices // *Appl. Surf. Sci.* – 2010. – V. 256. – P. 5263–5269.
9. Gun'ko V.M., Nychiporuk Y.M., Zarko V.I. et al. Relationships between surface compositions and properties of surfaces of mixed fumed oxides // *Appl. Surf. Sci.* – 2007. – V. 253. – P. 3215–3230.
10. Gun'ko V.M., Blitz J.P., Gude K. et al. Surface structure and properties of mixed fumed oxides // *J. Colloid Interface Sci.* – 2007. – V. 14. – P. 119–130.
11. Kaneko K., Sato N., Suzuki T. et al. Surface fractal dimension of microporous carbon fibres by nitrogen adsorption // *J. Chem. Soc. Faraday Trans.* – 1991. – V. 87. – P. 179–185.

12. Avnir D. The Fractal Approach to Heterogeneous Chemistry. – New York. – Chichester: Wiley, 1989. – 441 p.
13. Gregg S.J., Sing K.S.W. Adsorption, Surface Area and Porosity. – London: Academic Press, 1991. – 303 p.
14. Roquerol F., Roquerol J., Sing K. Adsorption by Powders and Porous Solids. Principles, Methodology and Applications. – London: Elsevier, 1999. – 467 p.
15. Nguyen C., Do D.D. A new method for the characterization of porous materials // Langmuir. – 1999. – V. 15. – P. 3608–3615.
16. Nguyen C., Do D.D. Effects of probing vapors and temperature on the characterization of micro-mesopore size distribution of carbonaceous materials // Langmuir. – 2000. – V. 16. – P. 7218–7222.
17. Voronin E.F., Gun'ko V.M., Guzenko N.V. et al. Interaction of poly(ethylene oxide) with fumed silica // J. Colloid Interface Sci. – 2004. – V. 279. – P. 326–340.
18. Borysenko M.V., Gun'ko V.M., Dyachenko A.G. et al. CVD-zirconia on fumed silica and silica gel // Appl. Surf. Sci. – 2005. – V. 242, N 1–2. – P. 1–12.
19. Bogatyrev V.M., Oranska O.I., Gun'ko V.M. et al. Influence of metal content on structural characteristics of inorganic nanocomposites M_xO_y/SiO_2 and $C/M_xO_y/SiO_2$ // Chemistry, Physics and Technology of Surface. – 2011. – V. 2, N 2. – P. 135–146 (in Russian).
20. Gun'ko V.M., Leboda R., Skubiszewska-Zięba J. Heating effects on morphological and textural characteristics of individual and composite nanooxides // Adsorption. – 2009. – V. 15, N 2. – P. 89–98.
21. Gun'ko V.M., Mikhalovsky S.V. Evaluation of slitlike porosity of carbon adsorbents // Carbon. – 2004. – V. 42, N 4. – P. 843–849.
22. Avnir D., Jaroniec M. An isotherm equation for adsorption on fractal surfaces of heterogeneous porous materials // Langmuir. – 1989. – V. 5. – P. 1431–1433.
23. Lowell S., Shields J.E., Thomas M.A., Thommes M. Characterization of Porous Solids and Powders: Surface Area, Pore Size and Density. – Dordrecht: Springer, 2004. – 350 p.
24. Jaroniec M., Kruk M., Olivier J. Fractal analysis of composite adsorption isotherms obtained by using density functional theory data for argon in slitlike pores // Langmuir. – 1997. – V. 13, N 5. – P. 1031–1035.
25. Jolly W.L. Modern Inorganic Chemistry. – New York: McGraw-Hill, 1984. – 610 p.
26. Pauling L. Nature of the Chemical Bond and the Structure of Molecules and Crystals. – New York: Cornell University Press, 1960. – 644 p.
27. Allen L.C. Electronegativity is the average one-electron energy of the valence-shell electrons in ground-state free atoms // J. Am. Chem. Soc. – 1989 – V. 111, N 25. – P. 9003–9014.

Received 15.10.2012, accepted 05.11.2012

**Вплив допування оксидами міді (II) та нікеля (II)
на морфологічні властивості нанокompозитів кремнезем/диоксид титану**

**М.О. Назарковський, О.В. Гончарук, Є.М. Пахлов, E. Skwarek,
J. Skubiszewska-Zięba, R. Leboda, W. Janusz, В.М. Гунько**

*Институт хімії поверхні ім. О.О. Чуйка Національної академії наук України
вул. Генерала Наумова, 17, Київ, 03164, Україна, nazarkovsky.michael@gmail.com
Університет імені Марії Кюрі-Склодовської, хімічний факультет
пл. Марії Кюрі-Склодовської, 3, Люблін, 20031, Польща*

За допомогою атомно-силової мікроскопії та за даними низькотемпературної адсорбції азоту проаналізовано морфологічні властивості титанокремнеземів, допованих CuO та NiO. Пори різних типів (класифіковані за розмірами як нано-, мезо- та макропори) розглядаються як порожнечі між сферичними частинками нанокompозитів, сформованими в агрегати. Показано, що питома поверхня, загальний об'єм пор, їх середній радіус, інкрементальний розподіл пор за розмірами та зміни у співвідношеннях між цими величинами композитів демонструють нелінійну поведінку, що є функцією присутності допанта. Результати дослідження текстури та дані атомно-силової мікроскопії дають підстави вважати, що процеси агрегування частинок різняться між собою в залежності від природи допуючого оксиду. Фрактальна розмірність, обчислена за рівнянням Френкеля-Хелсі-Хілла, варіюється між 2.50 та 2.60, що також свідчить про формування агрегатів.

**Влияние допирования оксидами меди (II) и никеля (II)
на морфологические свойства нанокompозитов кремнезем/диоксид титана**

**М.А. Назарковский, Е.В. Гончарук, Е.М. Пахлов, E. Skwarek,
J. Skubiszewska-Zięba, R. Leboda, W. Janusz, В.М. Гунько**

*Институт химии поверхности им. А.А. Чуйко Национальной академии наук Украины
ул. Генерала Наумова, 17, Киев, 03164, Украина, nazarkovsky.michael@gmail.com
Университет имени Марии Кюри-Склодовской, химический факультет
пл. Марии Кюри-Склодовской, 3, Люблин, 20031, Польша*

По данным атомно-силовой микроскопии и низкотемпературной адсорбции азота проанализированы морфологические свойства титанокремнеземов, допированных CuO и NiO. Пores различных размеров (нано-, мезо- и макропоры) рассматриваются как порожнечы между сферическими частицами нанокompозитов, формирующими агрегаты. Показано, что удельная поверхность, общий объем пор, их средний радиус, инкрементальное распределение пор по размерам, а также изменения в соотношениях этих величин демонстрируют нелінейное поведение в зависимости от допирующего оксиду. Результаты исследования текстуры и данные атомно-силовой микроскопии дают основание полагать, что природа допанта определяет различия в процессах агрегирования частиц. Фрактальная размерность, рассчитанная по уравнению Френкеля-Хелси-Хилла, изменяется от 2.50 до 2.60, что также свидетельствует о формировании агрегатов.